Pion scattering from spin $\frac{1}{2}$ nuclei

P. B. Siegel
California State Polytechnic University, Pomona, California 91768

W. R. Gibbs
New Mexico State University, Las Cruces, New Mexico 88003
and Los Alamos National Laboratory, Los Alamos, New Mexico 87545

(Received 10 May 1993)

Left-right asymmetries for pion elastic scattering and charge exchange from polarized ^{13}C and ^{15}N are calculated and compared with the available data. It is shown for elastic scattering that the quadrupole spin-flip contribution is dominant in the determination of the asymmetry at forward angles. The distorted wave impulse approximation and optical model treatments are compared and a qualitative discussion of the underlying physics of the sign of the asymmetry in the first diffraction minimum is presented.

PACS number(s): 25.80.Dj, 25.80.Ek, 24.70.+s, 24.10.Eq

I. INTRODUCTION

Over the past few years, pion scattering experiments from polarized nuclei have been successfully performed [1–3]. Measurements of the analyzing power on ^{6}Li, ^{13}C, ^{15}N, and ^{14}N for pion kinetic energies between 100 MeV and 220 MeV were done to better understand the spin-dependent components of the pion-nucleus interaction and the pion's interaction with the nucleus in general. Theoretical calculations have been largely unsuccessful in understanding the analyzing power measurements [4, 1, 3]. For elastic scattering on ^{13}C and ^{15}N, the predicted asymmetries are larger than the data and do not always have the correct sign. In this paper we report on a comprehensive analysis of pion scattering from polarized spin 1/2 nuclei. The asymmetry is calculated and compared with elastic scattering data from ^{13}C and ^{15}N as well as analog charge exchange data on ^{13}C.

Spin 1/2 nuclei are the least complicated to analyze, since there are only three distinct contributions to the scattering amplitude for elastic pion scattering and charge exchange to the isobaric analog state. These individual amplitudes are characterized by the amount of angular momentum transferred to the nucleus, and labeled $J(KS)$ following Ref. [5]. The integer J refers to the total angular momentum transfer, while K and S refer to the orbital and spin angular momentum transferred. For spin 0 and spin 1/2 particles in the initial and final states, the possiblities are the monopole nonflip 0(00), the monopole spin-flip 1(01), and the quadrupole spin-flip 1(21) pieces. We use this notation throughout the paper, and label the corresponding amplitudes as $f_{0(00)}$, $h_{1(01)}$ and $h_{1(21)}$. The complete spin-flip amplitude is defined as $h = h_{1(01)} + h_{1(21)}$. A left-right asymmetry is caused by an interference between the spin-flip and nonflip pieces. It is hoped that an understanding of the asymmetry from spin 1/2 nuclei will be a stepping stone to understanding more complicated inelastic processes and nuclei with larger spin.

We first compare the two principal methods that are used in calculating the asymmetry for spin 1/2 nuclei: the distorted wave impulse approximation (DWIA) and the spin-dependent optical potential approach. Then we discuss qualitative features of the left-right asymmetry in order to understand the important components which determine its magnitude and sign. Finally, we compare our calculations with the available data.

II. COMPARISON OF THE DWIA AND THE SPIN-DEPENDENT OPTICAL POTENTIAL

In this section we compare calculations using the DWIA with those using a spin-dependent optical potential. Calculations using both methods exist in the literature [4, 5]. For the purposes of this comparison only, we restrict the calculation to the 0(00) and 1(01) contributions. Without the quadrupole-flip 1(21) piece, the spin-dependent optical potential does not mix partial waves and the calculation is greatly simplified. When we compare to the data, the DWIA is used and the 1(21) contribution is of course included.

For the spin-dependent part of the optical potential we take the following form in momentum space:

$$V_{\rm spin}(\mathbf{k},\mathbf{k}') = it_{\rm SF}\rho_t(|\mathbf{k}-\mathbf{k}'|)\boldsymbol{\sigma}\cdot\mathbf{k}\times\mathbf{k}' , \tag{1}$$

where ρ_t is the transition density of the valence nucleon and $t_{\rm SF}$ is determined from the measured π-nucleon spin-flip amplitude.

Upon transformation to coordinate space, this potential becomes

$$V(\mathbf{r})\Psi(\mathbf{r}) = -it_{\rm SF}\boldsymbol{\sigma}\cdot\boldsymbol{\nabla}\times[\rho_t(\mathbf{r})\boldsymbol{\nabla}\Psi(\mathbf{r})] . \tag{2}$$

Expanding the derivatives gives

$$\begin{aligned} V(\mathbf{r})\Psi(\mathbf{r}) &= -it_{\rm SF}\boldsymbol{\sigma}\cdot[\boldsymbol{\nabla}\rho_t(\mathbf{r})\times\boldsymbol{\nabla}\Psi + \rho_t(\mathbf{r})\boldsymbol{\nabla}\times\boldsymbol{\nabla}\Psi] \\ &= -it_{\rm SF}\sigma\cdot\boldsymbol{\nabla}\rho_t(\mathbf{r})\times\boldsymbol{\nabla}\Psi, \end{aligned} \tag{3}$$

since Ψ is a scalar function. If $\rho_t(\mathbf{r})$ is spherically sym-

metric, the expression can be simplified further to give the desired spin-orbit interaction:

$$V(\mathbf{r})\Psi(\mathbf{r}) = -it_{\mathrm{SF}}\boldsymbol{\sigma}\cdot\frac{1}{r}\frac{d\rho_t}{dr}\mathbf{r}\times\boldsymbol{\nabla}\Psi$$
$$= t_{\mathrm{SF}}\frac{1}{r}\frac{d\rho_t}{dr}\boldsymbol{\sigma}\cdot\mathbf{r}\times\mathbf{p}\Psi = t_{\mathrm{SF}}\frac{1}{r}\frac{d\rho_t}{dr}\boldsymbol{\sigma}\cdot\mathbf{L}\Psi. \quad (4)$$

We see that when only the monopole spin-flip piece is included, the spin-dependent part of the potential can be expressed as a spin-orbit interaction which does not couple different angular momenta. The nonflip part of the optical potential, which represents scattering from the core, is described in Ref. [6] and is added to the spin-dependent part of Eq. (4) to form a complete optical potential for ^{13}C, which is then inserted into a truncated Klein-Gordon equation. The resulting scattering amplitudes are labeled as f_{l+} and f_{l-} for $j = l + \frac{1}{2}$ and $j = l - \frac{1}{2}$, respectively. The complete scattering amplitude is expressed as an operator in spin space by

$$F(\theta) = f(\theta) + h(\theta)\boldsymbol{\sigma}\cdot\hat{\mathbf{n}}\times\hat{\mathbf{n}}', \quad (5)$$

where

$$f(\theta) = \sum[(l+1)f_{l+} + lf_{l-}]P_l(\cos\theta) \quad (6)$$

and

$$h(\theta) = \sum(f_{l+} - f_{l-})P_l^1(\cos\theta), \quad (7)$$

and $\hat{\mathbf{n}}$ and $\hat{\mathbf{n}}'$ are unit vectors in the direction of the incident and outgoing pions, respectively. The left-right asymmetry, or analyzing power, is then given as

$$A_y = \frac{2\mathrm{Re}(fh^*)}{f^2+h^2} = \frac{2\mathbf{f}\cdot\mathbf{h}}{f^2+h^2}, \quad (8)$$

where $\mathbf{f}$ and $\mathbf{h}$ are vectors in the complex plane.

In the DWIA calculation, the spin-independent part of the potential, which represents scattering from the core, is inserted into the truncated Klein-Gordon equation. Distorted waves are generated and used to calculate the scattering amplitude from the valence nucleon via the following operator:

$$O_{\mathrm{DWIA}} = (t_0 + t_1\mathbf{q}\cdot\mathbf{q}' + t_{\mathrm{SF}}\boldsymbol{\sigma}\cdot\mathbf{q}\times\mathbf{q}')v(q)v(q'), \quad (9)$$

where the complex amplitudes t_0, t_1, and t_{SF} come from the free π-nucleon amplitudes. In the matrix element of this operator the vectors $\mathbf{q}$ and $\mathbf{q}'$ are treated as gradient operators. The form used for the off-shell form factor $v(q)$ is

$$v(q) = \frac{\alpha^2+k^2}{\alpha^2+q^2}, \quad (10)$$

where k is the on-shell momentum and α is a parameter which represents the range of the pion-nucleon interaction. For the calculations presented here we take $\alpha = 550$ MeV/c as suggested by a recent study of elastic scattering from the calcium isotopes [7]. For elastic scattering this amplitude is added to the amplitude from the core to give the full scattering amplitude, $f \pm h$. The left-right asymmetry is determined from Eq. (5).

Each of the approaches described above is an approximation in its own way. For example, the DWIA does not include the triple scattering: valence nucleon, core, valence nucleon. Iteration of the spin-dependent optical potential will include this contribution. However, it will also include the undesired contribution of scattering from the valence nucleon multiple times while propagating the ground state between scatterings. This could lead to false results when calculating asymmetries, with the largest errors occurring when the amplitude from the core is the smallest (i.e., in the minima of the differential cross section). We show a calculation of the extreme case in Fig. 1(a) where we have set the core potential to zero. The optical potential only includes the interaction with the valence nucleon and is of the form

$$V_{\mathrm{val}} = e(V_{\text{non-flip}} + V_{\text{spin-dependent}}), \quad (11)$$

where the quantity e has been introduced as a scaling factor. Ideally, the differential cross section should be equal to the free nucleon result multiplied by a diffraction form factor, since there is only one nucleon present. The asymmetry should be the same as the free case since the form factor will cancel in the ratio of amplitudes. For our example, we chose a π^- of kinetic energy 165

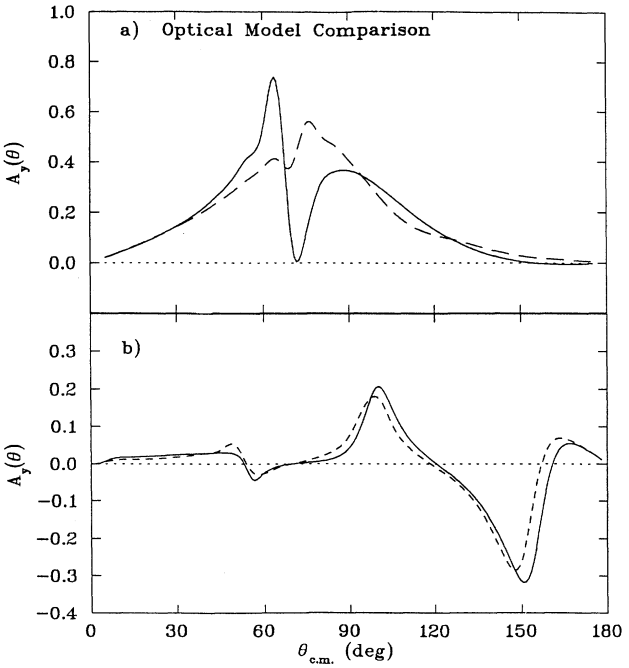

FIG. 1. (a) Comparison of the DWIA and optical model techniques for computing polarization asymmetry from a single particle with varying strength for the interaction. The solid curve is calculated for $e = 1$ and the dotted curve is for $e = 0.02$. The free case looks much like the dotted curve but has no inflection near the minimum in the nuclear differential cross section. (b) Comparison of the DWIA and optical model techniques for a realistic case of scattering from ^{15}N. The solid line is calculated with the distorted wave approach and the dotted line with the optical model. The monopole spin-flip potential has been enhanced by a factor of 3 for this comparison.

MeV scattering from the valence neutron of ^{13}C. When e equals unity, as shown in Fig. 1(a), the calculated asymmetry is very different than the free π^--neutron result. The difference is greatest near the diffraction minimum where multiple scattering is relatively large. By making e very small, 0.02, multiple scattering is reduced and approximate agreement is obtained with the free case. Thus, multiple scatterings from the valence nucleon without properly projecting out the ground state may lead to very incorrect results, particularly in calculating the left-right asymmetry.

In order to check the validity of the two methods for light nuclei, we compare calculations of the asymmetry for π^+ scattering from ^{15}N. The monopole spin-flip contributes very little to the asymmetry (see next section), and so, for this model comparison only, we increase the 1(01) strength by a factor of 3 to produce observable asymmetries. The results are shown in Fig. 1(b) for a pion kinetic energy of 132 MeV. The calculated asymmetries for the two methods agree very well. This is encouraging, since they are different approximations. At 165 MeV, where the diffraction minimum is deeper, the agreement is not as good. This is perhaps due to the spurious scattering from the valence nucleon discussed above. In all further calculations in this paper the DWIA is used, and all three components of the nuclear structure are included.

III. GENERAL FEATURES OF THE ASYMMETRY FOR ^{13}C AND ^{15}N

In this section we show that the quadrupole-flip contribution 1(21) is the principal contributor in determining the left-right asymmetry for elastic scattering at forward angles and discuss how the sign of the asymmetry changes through the first diffraction minimum using the DWIA. Choosing the z axis to be perpendicular to the scattering plane we can express the scattering amplitude as $f \pm h$. The differential cross section is given by $f^2 + h^2$, and the left-right asymmetry is given by Eq. (8). For elastic scattering from spin 1/2 nuclei, the 1(01) and 1(21) pieces add coherently to give h, whereas f is determined solely from the monopole nonflip 0(00) contribution.

One reason that the quadrupole spin-flip is so important in producing the asymmetry is that it is relatively large when the nonflip amplitude is small. This can be seen in Fig. 2, where we plot the differential cross-section contributions for each of the three pieces for elastic scattering of π^- from ^{13}C at 132 MeV. The 1(01) and 1(21) amplitudes add coherently, but we plot their absolute squares here separately for comparison. The asymmetry will be appreciable when h is comparable to f. As can be seen in the figure, the cross section from the monopole flip has a minimum at roughly the same angle as the 0(00) piece. This is because in both cases the minimum is due to a diffraction minimum in a monopole form factor. In the 0(00) case, the form factor is primarily from the core, and in the 1(01) piece the form factor arises from the transition density. Since these densities are not very different, the first diffraction minima are at nearly the same angle. The cross section due to the 1(21) contribution, on the other hand, is approximately proportional to $\sin\theta$ times the quadrupole form factor of the transition density and will have a different angular distribution from the 0(00) piece. Thus, it can be large when the 0(00) and 1(01) contributions are small and produce a left-right asymmetry in the cross section. The above arguments are generally valid for pion-nucleus scattering at energies near the resonance where the minima in the differential cross section are diffraction dominated. At lower energies, where the minima can be caused by an s-p interference, the monopole-flip amplitude might be important in producing asymmetries.

In the case of ^{13}C and ^{15}N the quadrupole amplitude is further enhanced over the monopole due to nuclear structure. If we consider the valence neutron in the $1p_{1/2}$ shell, which is the main component of the wave function, then the monopole spin-flip pion-nucleus amplitude is reduced by a factor of $-1/3$ from the free pion-nucleon value. A pure $p_{1/2}$ neutron for the initial and final states gives (see Appendix A), for the monopole-flip amplitude in the plane wave approximation,

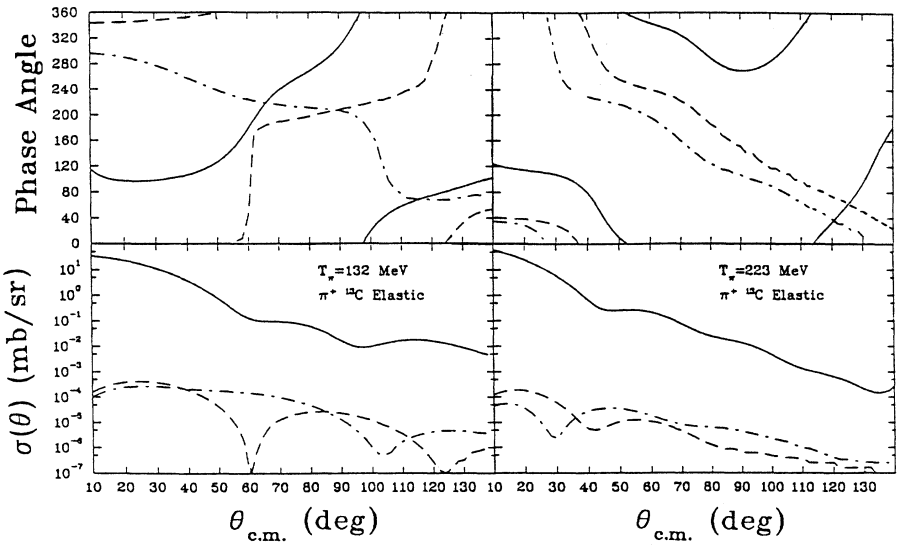

FIG. 2. Left: phase angle and cross sections from the monopole (solid), monopole spin-flip (dashed), and quadrupole spin-flip (dash-dotted) amplitudes for π^+ scattering at 132 MeV. Note that the phase angle of the mono pole pieces rotate counter clockwise through the first minimum. Right: phase angle and cross sections form the mono pole (solid), monopole spin-flip (dashed), and quadrupole spin-flip (dash-dotted) amplitudes for π^+ scattering at 223 MeV. Here the phase angles of the monopole pieces rotate clock wise through the first minimum.

$$h_{1(01)}(\theta) = -\frac{1}{3} i t_{\mathrm{SF}} \sin\theta \int_0^\infty \rho_t j_0(qr) r^2 dr. \quad (12)$$

The quadrupole spin-flip amplitude, for the plane wave approximation, on the other hand, is somewhat enhanced; a pure $p_{1/2}$ neutron gives (see Appendix A)

$$h_{1(21)}(\theta) = +\frac{2}{3} i t_{\mathrm{SF}} \sin\theta \int_0^\infty \rho_t j_2(qr) r^2 dr. \quad (13)$$

The currently available asymmetry data for ^{13}C and ^{15}N are between 100 MeV and 220 MeV, i.e., in the 33 resonance region. Thus the forward-angle left-right asymmetry in the differential cross section is primarily due to the quadrupole-flip transition for the two reasons discussed above. This is particularly true for elastic scattering where the 0(00) piece is primarily due to the core and is very large compared to the spin-dependent amplitude, h. In fact, when the monopole spin-flip piece is excluded in the elastic scattering calculations, there is practically no change in the left-right asymmetry in this energy region. For charge exchange, the situation is somewhat different, since the 0(00) amplitude itself comes only from the valence nucleon. The spin-independent and spin-dependent amplitudes are comparable and the monopole-flip contribution becomes more important.

The sign of the left-right asymmetry can be best analyzed by expressing the asymmetry as in Eq. (8):

$$A_y = \frac{2\mathbf{f}\cdot\mathbf{h}}{f^2+h^2} = \frac{2fh\,\cos(\phi_f - \phi_h)}{f^2+h^2}. \quad (14)$$

In this form, one can focus on the vectors (in the complex plane) $\mathbf{f}$ and $\mathbf{h}$ as they vary with angle. Their relative phase will determine the sign of the asymmetry. In Fig. 2 we show the phase of the amplitudes of $f_{0(00)}$, of $h_{1(01)}$, and of $h_{1(21)}$ as a function of angle for π^- elastic scattering from ^{13}C at a pion kinetic energy 132 MeV. Since the 1(21) amplitude is the most important component in determining the asymmetry, the relative phase between the 0(00) and 1(21) vectors will determine the sign of the asymmetry. For small angles, this relative phase is greater than 90° and the asymmetry is negative. As the scattering angle is increased through the monopole diffraction minimum, $f_{0(00)}$ rotates counterclockwise, while $h_{1(21)}$ varies little in phase. Thus, as the angle is varied through the diffraction minimum, the relative phase passes from less than $-90°$ to 0° to greater than $+90°$, and the sign of the asymmetry will go from negative to positive to negative.

This trend of the sign of the asymmetry to go from negative to positive to negative through the first diffraction minimum for elastic scattering of π^+ or π^- is seen in all of the calculations for energies less than the resonance. This is because the asymmetry starts off negative for small angles and $f_{0(00)}$ rotates counterclockwise through the minimum. The negative asymmetry for small angles can be traced to the relative phase of the pion-nucleon spin-independent versus spin-dependent amplitudes and the relative phase of the monopole versus quadrupole form factor. The counterclockwise rotation of $f_{0(00)}$ is due to the attractive nature of the pion-nucleus interaction for energies less than the resonance (see Appendix B). This sign changing pattern persists when the theoretical model parameters are varied. We changed the off-shell range and excluded nuclear medium effects in our calculations, and the pattern through the first diffraction minimum remained. The data, except for a few points, also follow this pattern.

For repulsive potentials, the $f_{0(00)}$ amplitude rotates clockwise. For pion kinetic energies above the resonance, the pion-nucleus potential is repulsive, $f_{0(00)}$ rotates clockwise, and we expect the behavior of the sign of the asymmetry to be different than for energies below the resonance. Our calculations indicate that the asymmetry does not change sign through the diffraction minimum in this energy region. The limited data that are available for energies above the resonance show this feature. We note that the counterclockwise (clockwise) rotation of the $f_{0(00)}$ amplitude before (after) the resonance has also been observed in pion scattering from polarized ^{3}He [8].

In summary, the forward angle left-right asymmetry for pion elastic scattering from $1p$ shell spin 1/2 nuclei for energies near the resonance is primarily due to the quadrupole spin-flip contribution of the scattering amplitude. For elastic scattering from ^{13}C and ^{15}N at energies between 100 and 180 MeV the asymmetry changes sign from negative to positive to negative as the angle varies through the first diffraction minima. For energies above the resonance the sign of the asymmetry does not change sign through the first minimum. These are qualitative features which characterize the general properties of the asymmetry. In the next section we calculate specific cases and compare with the data.

IV. CALCULATIONS AND RESULTS

The most extensive data for elastic scattering on polarized spin 1/2 nuclei is on ^{13}C at 132 MeV [1, 9]. Data were taken for π^+ and π^- for angles through the first and second minima. Calculations are shown in Fig. 3 along with the data. The pion-nucleus optical potential of Ref. [6] was used to obtain the elastic scattering amplitude from the ^{12}C core, while producing distorted waves for the DWIA calculation of the amplitude from the valence neutron. The radial wave function for the valence neutron was obtained from a Woods-Saxon potential by adjusting the potential strength until the binding energy of the neutron matched the experimental value. The nuclear reduced matrix elements were taken from Ref. [10]. In Figs. 3–5 two calculations are shown. The solid line is the result of using the first order optical potential of Ref. [6], and the dashed line is the result obtained by adding an imaginary potential proportional to ρ^2 to the first order optical potential to account for true pion absorption. The strength of the imaginary ρ^2 piece was adjusted so that the calculated true pion absorption cross section matched the experimental data. In both calculations, separate densities for the neutrons and protons for the ^{12}C core were used. To test the sensitivity to nucleon densities, we ran a calculation in which both the neutrons and protons in the ^{12}C core had the same Woods-Saxon

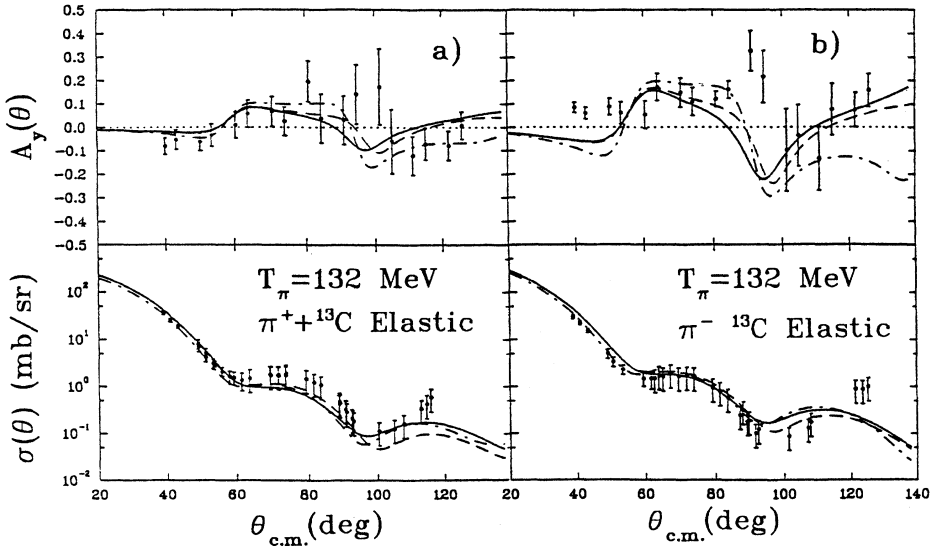

FIG. 3. Comparison with data for π^+ and π^- elastic scattering on ^{13}C at 132 MeV. The solid and dash-dotted lines are the results obtained from distorted waves computed with the pure first order optical potential. As explained in the text, the two curves correspond to different densities for the ^{13}C core. The dashed line is the result obtained by adding an imaginary potential proportional to ρ^2 to the first order optical potential to account for true pion absorption as was done in Ref. [7].

density. The results of this calculation are shown as the dash-dotted curve in Figs. 3(a) and 3(b). For the π^+ case, the calculations of the asymmetry agree very well with the data. The sign of the measured asymmetry changes from negative to positive to negative through the first diffraction minimum to maximum to minimum, and the calculations have this feature as discussed in the previous section. The magnitudes of the calculation are also in fair agreement with the data.

Often the asymmetry changes sign just before or just after a minimum in the cross section. Thus, if calculations of the differential cross section do not reproduce the same angular structure as the data, then asymmetry calculations with be out of phase with the experimental results. So we focus here on how the sign changes through minima and maxima of the differential cross section, rather than comparing angle by angle with the data. At 132 MeV the differential cross section calculation agrees well with the data, and the sign changes of the asymmetry match the experimental angles. For the π^- projectile the asymmetry calculation and data are similar to the π^+ case. The calculation and data agree well except for the first two angles, where the experimental asymmetry is not negative just before the first cross-section minimum. This is a bit puzzling, since the π^+ has a negative asymmetry before the first minima. The π^+ has a different Coulomb interaction and does not interact as strongly with the valence neutron, but we are unable to understand the difference in the asymmetries for these two forward angles.

The data [9] at 226 MeV for π^- and at 223 MeV for π^+ have an extended angular distribution which includes the first minimum to maximum to minimum of the differential cross section. Figure 4 shows the comparison of data and calculations. The calculations remain negative through the first minimum-maximum-minimum region as discussed above, but the data do become positive at the center of the maximum for both π^+ and π^-. The

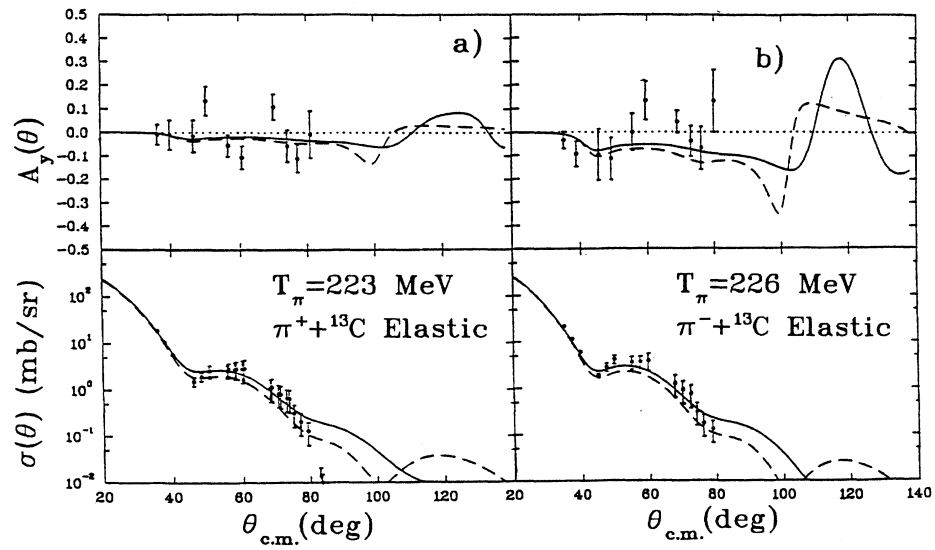

FIG. 4. Comparison with data for π^+ and π^- elastic scattering on ^{13}C at 223 (226) MeV. The solid and dashed lines have the same meaning as in Fig. 3.

asymmetries are small, and so it is difficult to draw any conclusions, but the calculations do become less negative, essentially zero, at the center of the maximum. Perhaps the calculated phase of $f_{0(00)}$ is not rotating at the correct angular rate in this region. The differential cross section agrees fairly well at these energies. It would be valuable to have data through the first diffraction minimum at other energies to investigate this property further.

At 114 MeV, there are asymmetry data for π^- at the start of the first maximum of the differential cross section. From the arguments of the previous section, we expect the sign of the asymmetry to go from negative to positive in this region. The experimental data show this feature. Calculations are presented along with the data in Fig. 5.

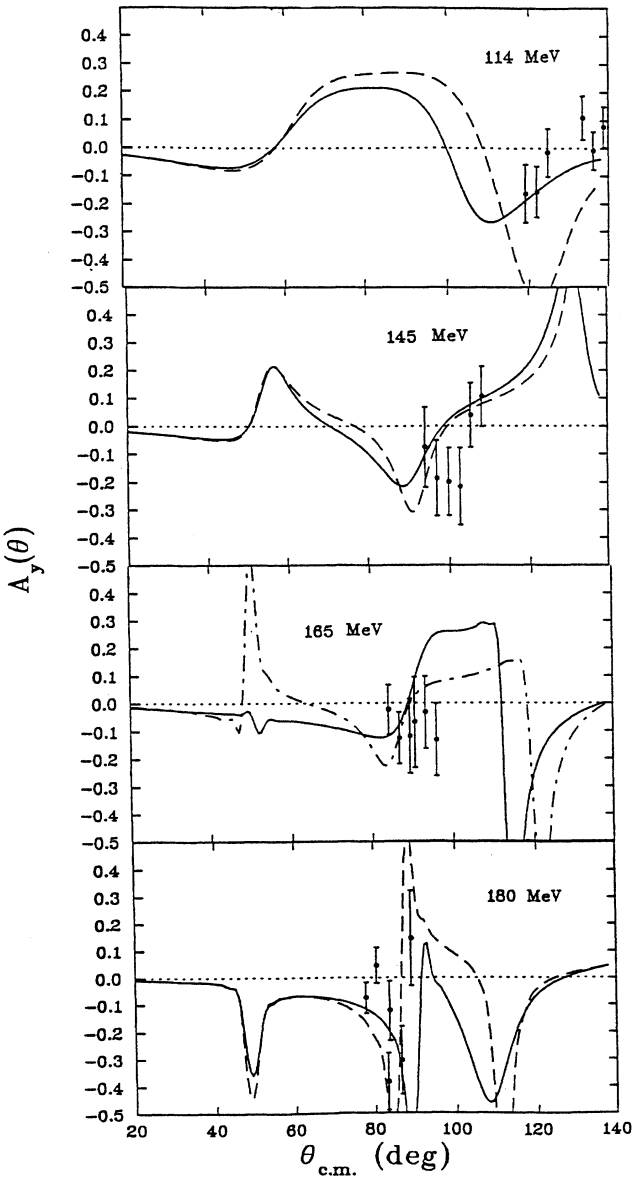

FIG. 5. Comparison with data for ^{13}C at 114, 145, 165, and 180 MeV. The solid and dashed lines have the same meaning as in Fig. 3.

A similar situation exist at 145 MeV, where data exist at the start of the first maximum and the sign of the asymmetry changes from negative to positive.

At 165 MeV and 180 MeV, limited data exist for π^- elastic asymmetry just after the first maximum of the cross section. In this region of the cross section the sign of the asymmetry is expected to be negative and turn positive in the second minimum. The data have this trend as shown in Fig. 5. It is difficult to match the second minimum of the cross section with only a first order optical potential. At 180 MeV the agreement is good and indeed one can make an angle-by-angle comparison with the asymmetry data. At 165 MeV, the second minimum of the calculated cross section occurs about 5° before the experimental minimum, and so one should compare the calculated asymmetries between 80° and 90° with the 85° to 95° data.

Thus, for elastic scattering, left-right asymmetry calculations using a first order optical potential to calculate the amplitude from the core and the DWIA for the amplitude from the valence neutron give good agreement with the data. The pattern of the sign change through the first minimum-maximum-minimum of negative to positive to negative to positive predicted for energies less than resonance is observed experimentally except for a few data points. This confirms a new property of the distorted waves previously untested, how the phase of the core amplitude varies with angle.

V. ELASTIC SCATTERING FROM ^{15}N

Calculations for elastic scattering of ^{15}N at 164 MeV are shown in Fig. 6. The calculations use the optical potential from Ref. [6] with the imaginary ρ^2 piece added in. The valence proton wave function was determined from a Woods-Saxon potential adjusted to match the experimental binding energy and the nuclear reduced matrix elements were taken from Ref. [10]. The experiment was done near the resonance energy, and the calculations indicate that the asymmetry stays negative through the first minimum-maximum-minimum region. The experimental asymmetry in this angular region is small, and

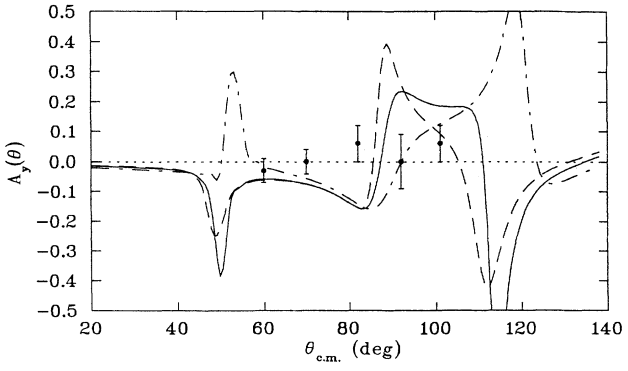

FIG. 6. Comparison with data for π^+ scattering on ^{15}N at 164 MeV. The solid line is calculated for 164 MeV (the experimental conditions) while the dashed line is for 170 MeV and the dash-dotted line is for 150 MeV.

not inconsistent with this result. The limited data show that the asymmetry might become positive in this region, similar to energies less than resonance. Since the sign of the asymmetry (at least at forward angles) changes from below to above the resonance and this experiment was performed very nearly on the resonance, it is possible that the small observed result might be anticipated if the energy were chosen to be exactly the crossover point. We varied the energy in our calculation to investigate the sensitivity of the asymmetry near the resonance energy, and found that the negative-positive-negative feature of the asymmetry through the first diffraction minimum persists until 150 MeV. It would be interesting to determine experimentally at what energy this transition occurs. We find, indeed, that at forward angles the asymmetry can be made zero by slight changes in the energy (or in other parameters difficult to control to the accuracy needed). However near 82° the predicted asymmetry is stable and larger than the data indicate. Thus we cannot explain the near-zero values observed at this one angle.

VI. CHARGE EXCHANGE FROM ^{13}C

The physics of the asymmetry from charge exchange is qualitatively different from that of elastic scattering. For a single valence neutron (as is the case of ^{13}C) both the non-spin-flip and spin-flip amplitudes arise from this single neutron. Thus, instead of a $1/A$ effect, as is seen in elastic scattering, we expect a polarization of the same order as that seen in charge exchange on the nucleon. This is indeed true and the agreement with both the cross section and the asymmetry at large angles is satisfactory. In the region of the first minimum there would appear to be a problem with the comparison of both observables. In order to rectify this disagreement, we varied the model parameters. Although unrealistic, elimination of the monopole-flip amplitude improves greatly the agreement with the data as shown in Fig. 7. For elastic scattering, elimination of the monopole-flip amplitude changed the asymmetry very little through the first diffraction minimum.

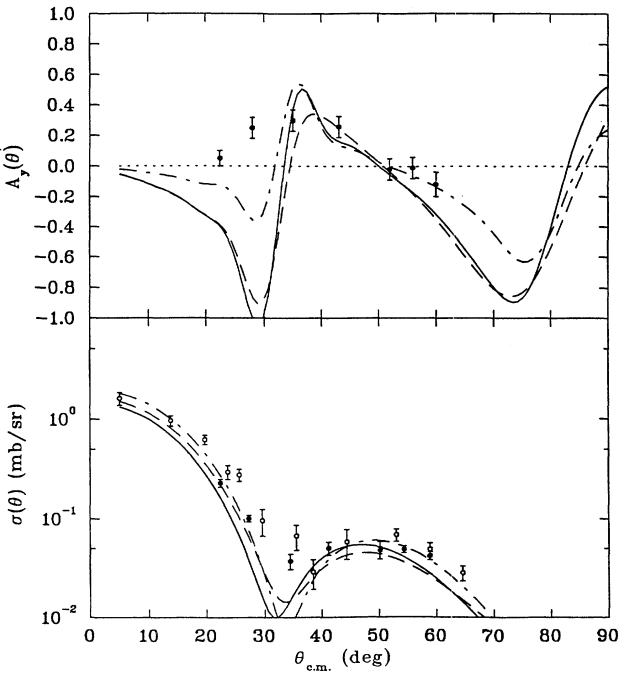

FIG. 7. Comparison with charge exchange data for ^{13}C at 163 MeV. The solid and dashed lines have the same meaning as in Fig. 3. The dash-dotted line is the result obtained by excluding the monopole spin-dependent contribution.

The $f_{0(00)}$ amplitude for charge exchange has a more complicated energy dependence than for elastic scattering. This is because at low energies the s- and p-wave amplitudes cancel in the forward direction [11]. This s-p interference makes A_y very sensitive to details of the pion-nucleus interaction. Thus, charge exchange asymmetry data for energies between 50 and 160 MeV would be valuable for a systematic study of how the pion interaction with the nucleus varies with energy.

VII. CONCLUSIONS

The DWIA and the spin-dependent optical potential approach were used to calculate the left-right asymmetry for pion scattering from ^{15}N in order to check the validity of the two methods. For this comparison the calculation was done at a pion kinetic energy of 132 MeV and only the monopole spin-flip amplitude was included for simplicity. The calculated asymmetries for the two methods agree very well, which is encouraging since they are different approximations. Using the DWIA we investigated qualitative features of the left-right asymmetry of pion scattering from polarized spin 1/2 nuclei for pion kinetic energies less than 240 MeV. For elastic scattering it is found that the asymmetry is mainly due to an interference between the monopole amplitude off the nuclear core and the quadrupole-flip amplitude from the valence nucleon. For ^{13}C and ^{15}N the phase of the core amplitude rotates counterclockwise for energies less than resonance and clockwise for energies greater than resonance. This property causes the asymmetry to vary with a certain pattern through the first diffraction minimum. For energies less than resonance the asymmetry changes from negative to positive to negative, and for energies greater than resonance the asymmetry remains negative through the minimum. The available data show roughly this behavior, confirming the variation of the core amplitude with angle, a property previously untested.

ACKNOWLEDGMENTS

We would like to thank Soumya Chakravarti and George Burleson for many helpful conversations about the theory and experiment. This work was supported in part by the United States Department of Energy and the Institute for Nuclear Theory at the University of Washington.

APPENDIX A

Here we review how nuclear structure favors the quadrupole spin-flip amplitude for a valence nucleon in

the $1p_{1/2}$ shell in the initial and final states. We choose the z axis along $\hat{\mathbf{n}} \times \hat{\mathbf{n}}'$. From the Bohr reflection theorem, if the initial nuclear state is polarized in the $+\hat{\mathbf{z}}$ direction, the final state will also be. The initial state of the valence nucleon is given by

$$\Psi_i = \sum_{m,\mu} \begin{pmatrix} 1 & \frac{1}{2} & \frac{1}{2} \\ m & \mu & \frac{1}{2} \end{pmatrix} \phi_1(r) Y_{1m}(\theta) |\tfrac{1}{2}\mu\rangle \tag{A1}$$

and similarly the final state of the valence nucleon is

$$\Psi_f = \sum_{m',\mu'} \begin{pmatrix} 1 & \frac{1}{2} & \frac{1}{2} \\ m' & \mu' & \frac{1}{2} \end{pmatrix} \phi_1(r) Y_{1m'}(\theta) |\tfrac{1}{2}\mu'\rangle, \tag{A2}$$

The ket $|\frac{1}{2}\mu\rangle$ represents the spin part of the nucleon wave function. In the plane wave approximation, the spin-dependent part of the scattering amplitude $h(\theta)$ can be expressed as

$$h(\theta) = it_{\mathrm{SF}} \sin\theta \sum_{m,m',\mu,\mu'} \langle \mu' | \sigma_0 | \mu \rangle \begin{pmatrix} 1 & \frac{1}{2} & \frac{1}{2} \\ m & \mu & \frac{1}{2} \end{pmatrix} \begin{pmatrix} 1 & \frac{1}{2} & \frac{1}{2} \\ m' & \mu' & \frac{1}{2} \end{pmatrix} \int \phi_1(r) \phi_1'(r) e^{i\mathbf{q}\cdot\mathbf{r}} Y_{1m} Y^*_{1m'} d^3r, \tag{A3}$$

where θ is the scattering angle. After expanding $e^{i\mathbf{q}\cdot\mathbf{r}}$ in a spherical basis, the expression becomes

$$h(\theta) = 4\pi i t_{\mathrm{SF}} \sin\theta \sum_{K,M,m,\mu,m',\mu'} i^K Y_{KM}(\hat{\mathbf{q}}) \int \rho_t(\mathbf{r}) \mathbf{j_K}(\mathbf{qr}) \mathbf{r^2 dr} \int \mathbf{Y^*_{KM}\ Y^*_{1m'}\ Y_{1m}\ d\Omega}$$
$$\times \langle \mu' | \sigma_0 | \mu \rangle \begin{pmatrix} 1 & \frac{1}{2} & \frac{1}{2} \\ m & \mu & \frac{1}{2} \end{pmatrix} \begin{pmatrix} 1 & \frac{1}{2} & \frac{1}{2} \\ m' & \mu' & \frac{1}{2} \end{pmatrix}. \tag{A4}$$

Upon integrating over angle and summing over M, m, m', μ, and μ' we obtain

$$h(\theta) = 6it_{\mathrm{SF}} \sin\theta \sum_K i^K \sqrt{4\pi(2K+1)} Y_{K0}(\hat{\mathbf{q}}) \int \rho_t(r) j_K(qr) r^2 dr \left[\begin{pmatrix} 1 & 1 & K \\ 0 & 0 & 0 \end{pmatrix}^2 \begin{pmatrix} 1 & 1/2 & 1/2 \\ 0 & 1/2 & -1/2 \end{pmatrix}^2 \right.$$
$$\left. + \begin{pmatrix} 1 & 1 & K \\ -1 & 1 & 0 \end{pmatrix} \begin{pmatrix} 1 & 1 & K \\ 0 & 0 & 0 \end{pmatrix} \begin{pmatrix} 1 & 1/2 & 1/2 \\ 1 & -1/2 & -1/2 \end{pmatrix}^2 \right]. \tag{A5}$$

For p-shell nucleons, the only K values which contribute are 0 and 2. Since $\hat{\mathbf{q}}$ lies in the scattering plane, $Y_{K0}(\hat{\mathbf{q}})$ is equal to $\sqrt{(2K+1)/(4\pi)} P_K(0)$. Explicitly carrying out the sum for $K = 0$ and $K = 2$ one obtains

$$h(\theta) = it_{\mathrm{SF}} \sin\theta \left[-\frac{1}{3} \int \rho_t(r) j_0(qr) r^2 dr + \frac{2}{3} \int \rho_t(r) j_2(qr) r^2 dr \right]. \tag{A6}$$

The above equation indicates that the quadupole spin-flip contributes more than the monopole in the plane wave approximation if the valence nucleon is in a pure $1p_{1/2}$ state. How pure a $1p_{1/2}$ state is the valence neutron? For a $1p_{1/2}$ state, the reduced matrix element is given by

$$\langle J_f = \tfrac{1}{2} \| (b \times b)_{1(K1)} \| J_i = \tfrac{1}{2} \rangle = 3\sqrt{2}\sqrt{2K+1} \begin{Bmatrix} K & 1 & 1 \\ 1 & 1/2 & 1/2 \\ 1 & 1/2 & 1/2 \end{Bmatrix}. \tag{A7}$$

For $K = 0$ this reduced matrix element is $-1/\sqrt{18} = -0.236$, and for $K = 2$ it is $\sqrt{10}/3 = 1.054$. These values agree well with Ref. [10], which lists these values for ^{15}N and -0.235 and 0.929, respectively, for a neutron in ^{13}C. However, this work limited their shell model basis to the p shell.

APPENDIX B

The rotation of the $f_{0(00)}$ amplitude is important in determining how the sign of the asymmetry changes through the first minimum, and can be understood by examining how the S matrix varies with partial wave. It is easiest to consider first an interaction described by a real potential in which the Coulomb interaction is neglected. For a complex potential, as in the case here, the results are qualitatively similar. For a real potential, the scattering is entirely elastic, and the scattering amplitude is given by

$$f_{0(00)} = \sum (2l+1) e^{i\delta_l} \sin\delta_l P_l(\cos\theta). \tag{B1}$$

For an attractive potential, but not so attractive as to cause a resonance, the phase shift δ_l starts off at some angle between 0° and 180,° at $l = 0$ and decreases to zero as the partial wave l increases. Thus the S matrix, and consequently $e^{i\delta_l}$, rotates clockwise on the unitary circle to the point (1,0) as l is increased.

At $\theta = 0$, the Legendre polynomials in Eq. (B1) are unity and the contribution from each partial wave is given the same weight. The amplitude $f_{0(00)}$ lies somewhere in the complex plane. As θ is increased, the Legendre polynomials decrease, except $l = 0$, with the larger l's decreasing faster. Thus, as the angle is increased, the contribution to the scattering amplitude from the larger partial waves decreases, the lower partial waves are weighted more, and the phase of $f_{0(00)}$ rotates counterclockwise.

In the case of a repulsive potential, the situation is reversed. The phase shift δ starts off at a negative angle between 0° and −180 ° for $l = 0$ and increases to zero as l increases. The S matrix and $e^{i\delta_l}$ will therefore rotate counterclockwise on the unitary circle as l is increased. When the angle θ is increased and the contribution from the larger partial waves decreases, the phase of $f_{0(00)}$

rotates clockwise.

These features have been verified for a real potential of Woods-Saxon shape for light nuclei and energies in the range of interest here. The inclusion of a complex piece of the optical potential causes the S matrix to lie inside the unitary circle, but the rotation of S with l is the same as with the real potential. The counterclockwise rotation of $f_{0(00)}$ at 132 MeV from 20° to 140° and the clockwise rotation at 223 MeV from 10° to 90° can be seen in Fig. 2.

In Fig. 2, it is also seen that the $f_{1(01)}$ amplitude, which comes from the DWIA, has the same rotation pattern with angle as the $f_{0(00)}$ piece. This can be understood again by referring to the case of the real potential. For a real potential, the wave function is given by

$$\Psi(r) = \sum i^l \psi_l Y_{lm}(\hat{\mathbf{r}})\ Y^*_{lm}(\hat{\mathbf{k}}) = \sum i^l e^{i\delta_l} \psi^r_l(r) Y_{lm}(\hat{\mathbf{r}})\ Y^*_{lm}(\hat{\mathbf{k}}), \quad \text{(B2)}$$

where δ_l is the phase shift of the lth partial wave, and $\psi^r_l(r)$ is a real function. In the DWIA, the $f_{1(01)}$ amplitude is given by Ref. [5]:

$$f_{1(01)} = \frac{i}{2\sqrt{(3)}} \langle f||\sigma||i\rangle \sum (2l+1) P^1_l(\cos\theta) \times \int (\psi_l)^2 \left(\frac{1}{r}\frac{d\rho_t}{dr}\right) r^2 dr. \quad \text{(B3)}$$

Substituting Eq. (B2) into (B3) we have

$$f_{1(01)} = \frac{i}{2\sqrt{3}} \langle f||\sigma||i\rangle \sum e^{2i\delta_l} (2l+1) P^1_l(\cos\theta) \times \int (\psi_l)^2 \frac{d\rho_t}{dr} r dr. \quad \text{(B4)}$$

Comparing Eq. (B4) with Eq. (B1) one can see that the phase of the $f_{1(01)}$ amplitude will behave in a similar manner to that of $f_{0(00)}$. That is, at zero degrees the phases of the high partial waves are strongly weighted, but as the scattering angle is increased the phases of the lower partial waves dominate. Thus for an attractive potential in which $e^{2i\delta_l}$ rotates clockwise with l, the amplitude $f_{1(01)}$ will rotate counterclockwise with angle as with $f_{0(00)}$. For a repulsive potential the situation is reversed.

For the $f_{1(21)}$ amplitude the situation is complicated by the fact that partial waves of $l \pm 2$ can contribute in the DWIA. We emphasize that the general features of the monopole amplitudes given in this appendix apply as the angle is varied through the first minimum only, and that numerical investigations were made only for the conditions of the experimental data.

[1] Yi-Fen Yen, B. Brinkmöller, D. Dehnhard, S. M. Sterbenz, Yi-Ju Yu, Brian Berman, G. R. Burleson, K. Cranston, A. Klein, G. S. Kyle, R. Alarcon, T. Averett, J. R. Comfort, J. J. Görgen, B. G. Ritchie, J. R. Tinsley, M. Barlett, G. W. Hoffmann, K. Johnson, C. F. Moore, M. Purcell, H. Ward, A. Williams, J. A. Faucett, S. J. Greene, J. J. Jarmer, J. A. McGill, C. L. Morris, S. Penttilä, N. Tanaka, H. T. Fortune, E. Insko, R. Ivie, J. M. O'Donnell, D. Smith, M. A. Khandaker, and S. Chakravarti, Phys. Rev. Lett. **66**, 1959 (1991).

[2] J. J. Görgen, J. R. Comfort, J. R. Tinsley, T. Averett, J. DeKorse, B. Franklin, B. G. Ritchie, G. Kyle, A. Klein, B. Berman, G. Burleson, K. Cranston, J. A. Faucett, J. J. Jarmer, J. N. Knudson, S. Pentilä, N. Tanaka, B. Brinkmöller, D. Dehnhard, Yi-Fen Yen, S. Høibråten, H. Breuer, B. S. Flanders, M. A. Khandaker, D. L. Naples, D. Zhang, M. L. Barlett, G. W. Hoffmann, and M. Purcell, Phys. Rev. Lett. **66**, 2193 (1991).

[3] R. Tacik, E. T. Boschitz, R. Maier, S. Ritt, M. Wessler, K. Junker, J. A. Konter, S. Mango, D. Renker, B. Brandt, W. Meyer, W. Thiel, P. Chaumette, J. Deregel, G. Durand, J. Fabre, P. A. Amaudruz, R. R. Johnson, G. R. Smith, P. Weber, and R. Mach, Phys. Rev. Lett. **63**, 1784 (1989).

[4] R. Mach and S. S. Kamalov, Nucl. Phys. **A511**, 601 (1990).

[5] P. B. Siegel and W. R. Gibbs, Phys. Rev. C **36**, 2473 (1987).

[6] W. B. Kaufmann and W. R. Gibbs, Phys. Rev. C **28**, 1286 (1983).

[7] W. R. Gibbs and J.-P. Dedonder, Phys. Rev. C **46**, 1825 (1992).

[8] C. B. Bennhold, B. K. Jennings, L. Tiator, and S. S. Kamalov, Nucl. Phys. **A540**, 621 (1992).

[9] Yi-Fen Yen, Ph.D. thesis, University of Minnesota, 1992; (unpublished).

[10] T.-S. H. Lee and D. Kurath, Phys. Rev. C **21**, 293 (1980).

[11] P. B. Siegel and W. R. Gibbs, Phys. Rev. C **33**, 1407 (1986).